CHAPTER - III

CHAPTER III

STUDIES ON ELECTRICAL, STRUCTURAL AND OPTICAL PROPERTIES OF PbS:CuS MIXED THIN FILMS

3.1 Introduction

As our goal is to develop a semiconductor material with properties suitable for photoelectrochemical applications, it will be of worthy if it is suitably prepared and thoroughly characterised through various techniques to understand its macroscopic behaviour.This chapter is fully devoted to the details of the deposition procedure and characterisation of the PbS and PbS:CuS samples through electrical, structural and optical properties. The preliminary key precautions to be taken while fabricating the material are discussed in the sections 2.2 and 3.2.1. Sections 2.3 and 3.2 respectively deals with the basic knowledge of the different characterisation techniques.The section 3.3 highlights some of the experimental observations on electrical transport, structural and optical properties of both PbS and PbS:CuS thin films.

3.2 Experimental Details

3.2.1 Deposition of the mixed PbS:CuS thin films

The preparation procedure and mechanism of the film formation for PbS:CuS mixed thin films are presented in the section 2.2. The method involves a reaction container consisting of equimolar solutions of lead acetate, sodium hydroxide and thiourea.The total volume of the solution was made up to approximately two third volume of a beaker by adding a double distilled water. Thoroughly cleaned glass slides were adjusted vertically in a beaker and a controlled quantity of copper sulphate solution was added directly into the lead acetate solution. The samples were taken out from the beaker and kept in a dark desiccator for further processings.

3.2.2 Electrical studies

a) Electrical conductivity

The dc electrical conductivity of the samples was measured in the 300K - 550K temperature range. Silver paint was applied to the samples for ohmic contacts /1,2/. A regulated dc power supply was used to pass the current through the sample and was measured with a HIL-2665, 4 1/2 digit currentmeter. For details refer section 2.3.3 of the chapter II.

b) Thermoelectric power

The thermo e.m.f.'s /3/ generated by the samples were measured in the range of temperature from 300K - 550K. Silver paint was applied to the samples and copper press contacts were drawn from the samples. The temperature difference was recorded by a Cr-Al thermocouple. The sensitive HIL-2665, 4 1/2 digit and Agronic-113 4 1/2 digit microvoltmeters were used to measure the thermovoltage and thermal gradients, respectively. The details of the thermopower measurements are summarised in section 2.3.4.

3.2.3 Structural and microscopic studies

a) XRD studies

The structural investigations were made using the X-ray diffraction technique. The angle range of scanning (2Θ) was from 5°-100° (CuK_α line).

b) SEM studies

The surface topography of the samples was observed through a Stereoscan, 250 MK(III), Camb Instrument (UK), Scanning Electron Microscope.

3.2.4 Optical studies

The optical absorption measurements were conducted on these samples in the 5000 A° - 26000 A° wavelength range to determine the absorption coefficient, nature of the transition and the energy band gap. A Hitachi-330, dual beam photospectrometer was utilised for this purpose.

3.3 Results and Discussion

3.3.1 Physical properties

The preparation of metal chalcogenide thin films is now fairly understood /1,2,4-11/. In the present case sodium hydroxide was used to give a solution pH of about 10.5. Sodium hydroxide also controls the rate of release of sulphur. The reaction mixture develops a white precipitate which gradually turns through yellow to brown and finally greyish black and the deposition of PbS on glass surface takes place during this process. The above processes can be chemically represented and are reproduced as /2,12/;

$$\begin{matrix} H_2N \\ \quad\backslash \\ \quad C = S \\ \quad / \\ H_2N \end{matrix} + O^-H \Longrightarrow SH^- + \begin{matrix} H_2N \\ \quad\backslash \\ \quad C = O \\ \quad / \\ H_2N \end{matrix} \qquad \ldots(3.1)$$

$$SH^- + O^-H \Longrightarrow H_2O + S^{2-} \qquad \ldots(3.2)$$

$$Pb\,(CH_3COO)_2 + S^{2-} \Longrightarrow PbS + 2\,CH_3COO^- \qquad \ldots(3.3)$$

The controlled quantities of copper sulphate solution were added in the reaction bath for the preparation of PbS:CuS films. Good quality samples with changing pleasant colours have been obtained for varying concentration of Cu in PbS /2,5/. The thickness of the sample is found to be decreased with an increased Cu-concentration. Typically the thickness varies from 0.58 μm to 0.12 μm as the Cu-concentration (X) is varied from 0 to 0.8. Figure 3.1 is a sketch of layer thickness (t) vs the copper concentration (X).

3.3.2 Electrical properties

a) Electrical conductivity

The electrical conductivity measurements showed increase in conductivity of the samples with increase in temperature indicating the semiconducting nature of the samples. The temperature dependence of the conductivity is shown in figure 3.2 for six typical samples. The increase of conductivity with temperature may obviously be due to increase in both carrier concentration and mobility /2,13/. The thermally activated electrical conductivity is;

$$\sigma = \sigma_o \exp(-Ea/KT) \qquad ...(3.4)$$

where, Ea is the activation energy, σ is the conductivity of the sample at any temperature T, σ_o is the conductivity at room temperature, K is the Boltzmann's constant and T is the absolute temperature. The variation of log σ with reciprocal of the temperature is almost linear and the activation energy of an electrical conduction has been determined from this linear region. The activation energy did not varied much with the Cu-concentration, however, variation of logarithmic conductivity with Cu-concentration is notable /2,11/. This is shown in figure 3.3. Initially the conductivity is found to be increased with the addition of Cu-content in PbS upto 0.075 mol% of copper and

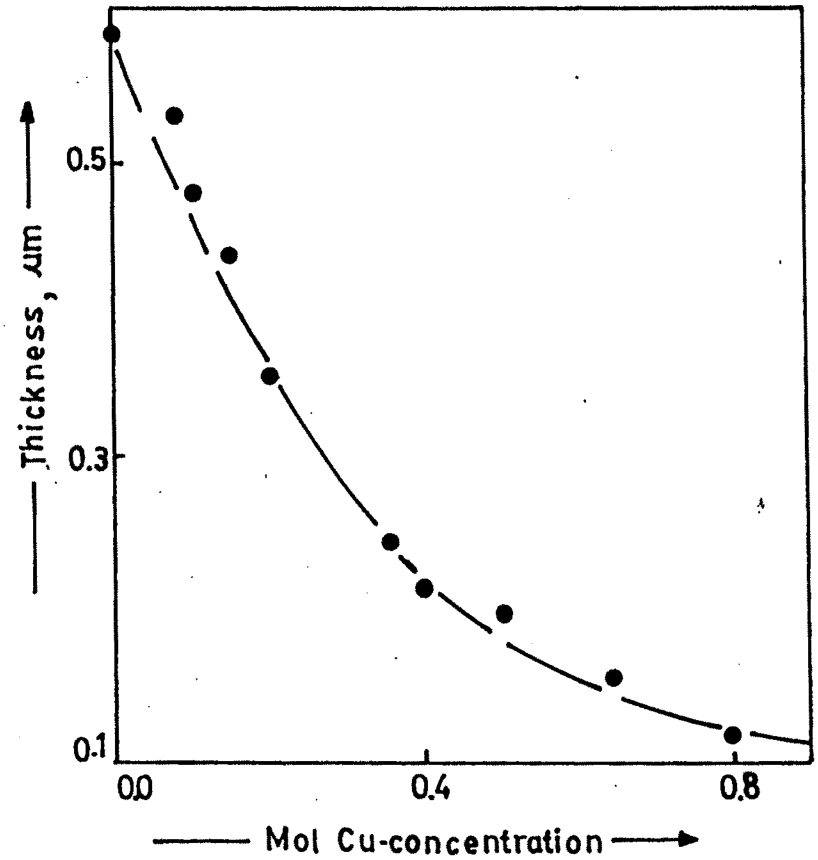

Fig. 3.1 Variation of thickness with the Cu – concentration in PbS thin film layer.

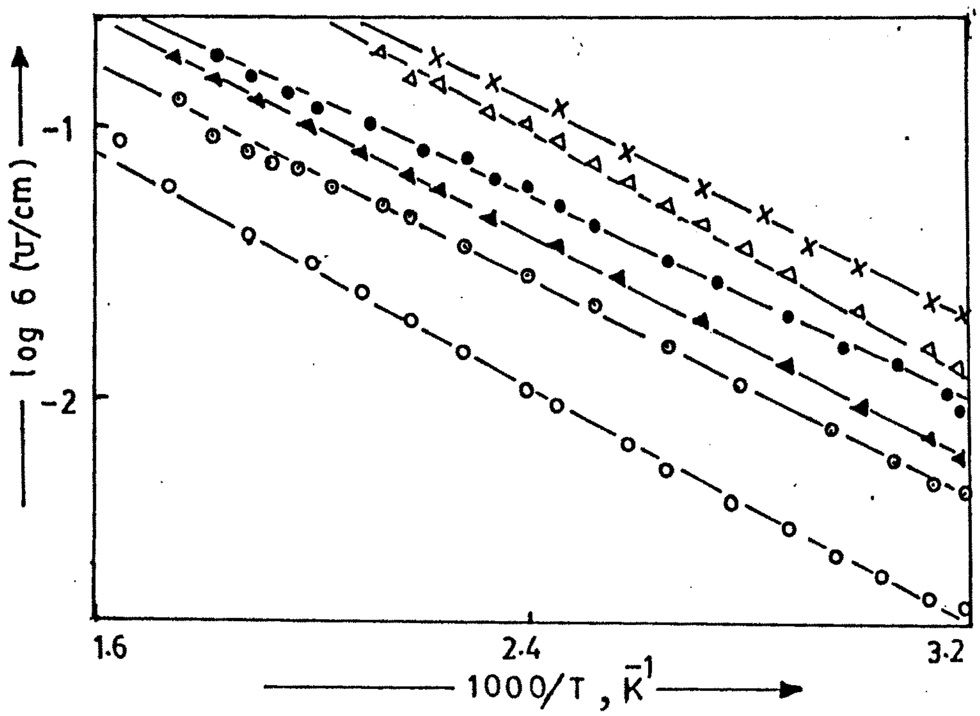

Fig. 3.2 Temperature dependence of conductivity : O ⟶ X = 0, ● ⟶ X = 0.05, Δ ⟶ X = 0.075, ⊙ ⟶ X = 0.1, ▲ ⟶ X = 0.15, x ⟶ X = 0.2.

further increase in Cu content upto 0.125 mol% causes a decrease in conductivity which again increases by further addition of Cu-concentration reaching a saturation beyond x = 0.2 /2,11/. An increase in conductivity for smaller concentration (upto 0.075 mol%) is assumed to be due to an increase in the number of free carriers supplied by Cu-ions /2,11,12/. Further increase in Cu - concentration (from 0.075 to 0.125 mol% of Cu) causes the copper ions to react with sulphur ions to form cupric sulphide phase, thus reducing the number of Cu-ions available for conduction /2,11/. This is seen from the decreased conductivity in this concentration range. As most of the charge carriers are utilised in bonding a new phase, a small number of free carriers are available for conduction which obviously shows decrease in conductivity to a value between PbS and CuS. The final increase in conductivity may be assigned to a little bit increased crystallinity that reduces the scattering of the carriers and thereby increasing the mobility/2,11,12/.

b) Thermoelectric (TEP) power

The thermoelectric voltages developed by the samples are positive towards the hot end of the sample. This shows that the holes are dominant carriers and that the conduction is p-type. Figure 3.4 shows the variation of thermoelectric power with temperature for three typical compositions. It is seen that thermoelectric power increases with temperature and is of the order of μV/K. The thermoelectric power (P) is related to the temperature (T) as /3/;

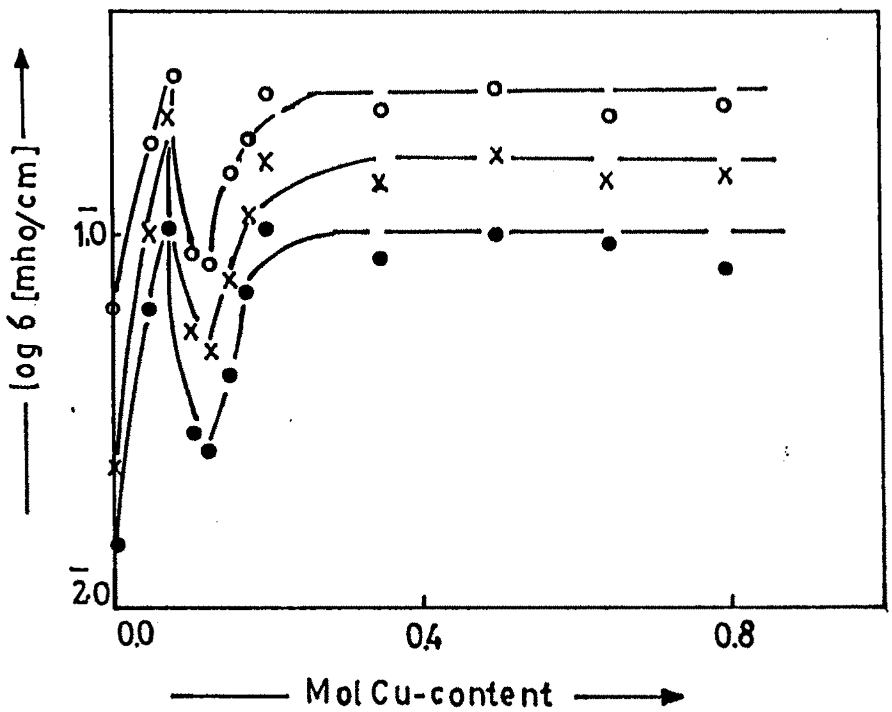

Fig. 3.3 Variation in conductivity with Cu - content for three typical temperatures :
O ⟶ 548K, X ⟶ 468K, ● ⟶ 418K

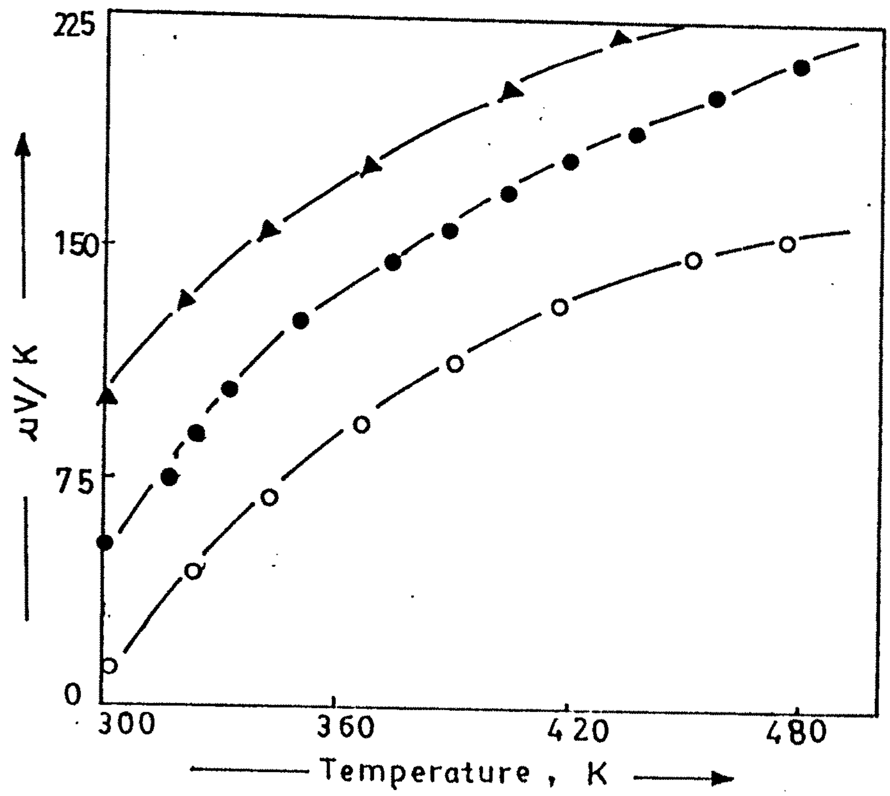

Fig. 3.4 Variation of thermoelectric power with temperature :
● ⟶ X = 0, ▲ ⟶ X = 0.075 and O ⟶ 0.65.

$$P = \pm \frac{K}{q} \left[A + \ln \frac{2(2\, m^*_e KT)^{3/2}}{nh^3} \right] \qquad \ldots(3.5)$$

where, q is the electronic charge, h is the Plank's constant, A is the thermoelectric power factor determined by the kinetic energy of electrons which depends on the scattering process, n is the carrier concentration, m^*_e is the effective mass of an electron, K is the Boltzmann's constant and T is the absolute temperature. It is also reported that at room temperature, The value of the thermoelectric power in PbS crystals obeys the following empirical relation over a range of carrier concentration extending from 10^{17} to 10^{19} cm^{-3} /13/;

$$P = \pm 200 \; [19.4 - \log n) \qquad \ldots(3.6)$$

If we use observed thermoelectric power at room temperature in equation 3.6 to evaluate the carrier concentration, we get a corresponding room temperature carrier concentration of the order of 10^{19} cm^{-3}. This is very similar to the results reported by George et al /13/ for PbS films prepared by reactive evaporation and by Bytenskii et al /14,15/ and Gudkin et al for PbSe polycrystalline films by vacuum evaporation. The carrier concentration (n) is calculated using the relation (3.6) and its dependence on Cu concentration is shown in figure 3.5. This characteristic is similar to that observed for the variation of conductivity for Cu content up to about 0.125 mol%. At higher Cu-concentration (>0.125), carrier concentration decreases initially and then again increases upto x=0.2 mol%. Further increase in copper concentration causes a decrease in the carrier density /2,11/. At such higher levels the interaction of Cu-atoms

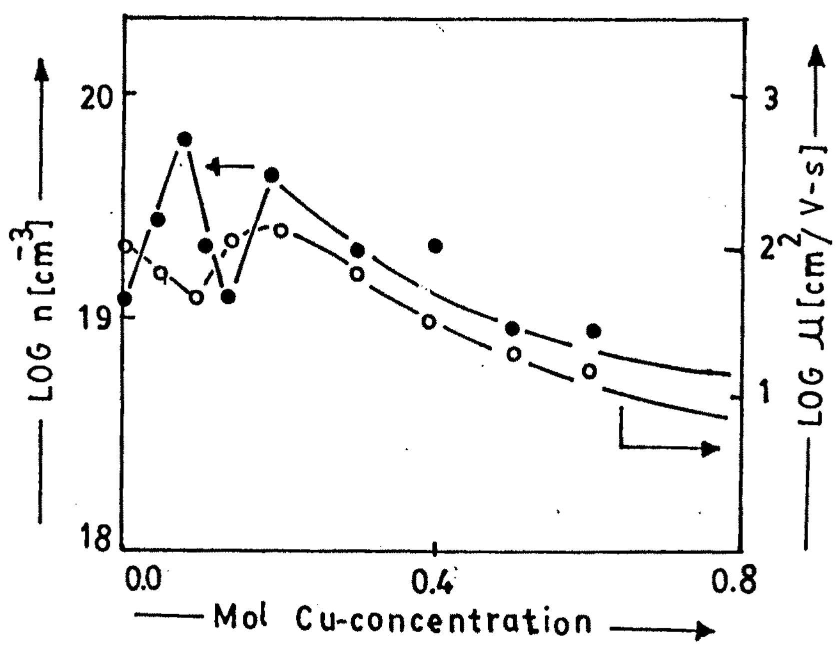

Fig. 3.5 Variation of carrier concentration and mobility with the Cu - concentration in PbS.

and host (PbS) atoms and scattering of carriers is likely to take place and also trapping of carriers at the grain boundaries and new energy levels causes decrease in the carrier concentration /11/. The data on electrical conductivity and thermoelectric power have been utilised to calculate the carrier mobility (u) following the usual relation;

$$\mu = \frac{\sigma}{n.e} \qquad \ldots(3.7)$$

where, μ is the carrier mobility in cm^2/VS, σ is the electrical conductivity in mho. cm and n is the carrier concentration $/cm^3$. Figure 3.5 shows the variation of mobility with the Cu-concentration in PbS. For low doping levels, this behaviour is also similar to the one observed for electrical conductivity. Initially the mobility decreases due to the increased carrier concentration. At higher Cu-concentration levels, the carrier density decreases reducing the scattering of the carriers and thereby increasing the carrier mobility /2,11/.The decrease in mobility at excessively higher values of x can be correlated, in our case, with the reduced grain size of the crystallites. The variation of mobility with temperature has also been studied. The mobility increases sharply as the temperature is increased. This is typical of many polycrystalline films and is due to the existence of potential barriers at the grain boundaries so called grain boundary potential or simply grain barrier height. Further, mobility in such cases is temperature activated and obeys a law of the form /13/;

$$\mu = \mu_o T^{-1/2} \exp\left(\frac{-\Phi_B}{KT}\right) \qquad \ldots(3.8)$$

where, Φ_B is the height of the potential barrier at the grain boundary. Φ_B is determined from the variation of log $\mu T^{1/2}$ vs 1/T. For pure PbS, Φ_B is of the order of 0.10 eV and it is 0.068 eV for 0.075 mol% CuS:PbS samples. This barrier height is of the same order as that obtained by several authors in chemically deposited PbS films /16,17/.

3.3.3 Structural properties

a) X-ray diffraction studies

The structure and degree of crystallinity for the samples were tested by XRD studies in the span of angles from 5°-100°. The X-ray diffractograms of four typical samples are shown in figure 3.6. The d values for the various peaks have been compared with the standard d values /18,19/. It is found that all the samples are crystalline in nature and the sample with x=0 consists of cubic phase of PbS while the samples with Cu-concentration consist of CuS hexagonal phase in addition to the cubic PbS phase /2/.Thus in our case the formation of new CuS phase has been detected. This contradicts the observations of Sharma et al /11/ where in they pointed out the formation of new alloyed phase of Cu_2S and PbS identified as (400), (420) and (422) reflections. However, analysis of our XRD data shows that the CuS and PbS phases form separately and a good fit is observed between the ASTM and the experimentally observed results /2,18,19/. The reflections (400), (420) and (422) are due to the cubic PbS only and it is interesting to note that addition of

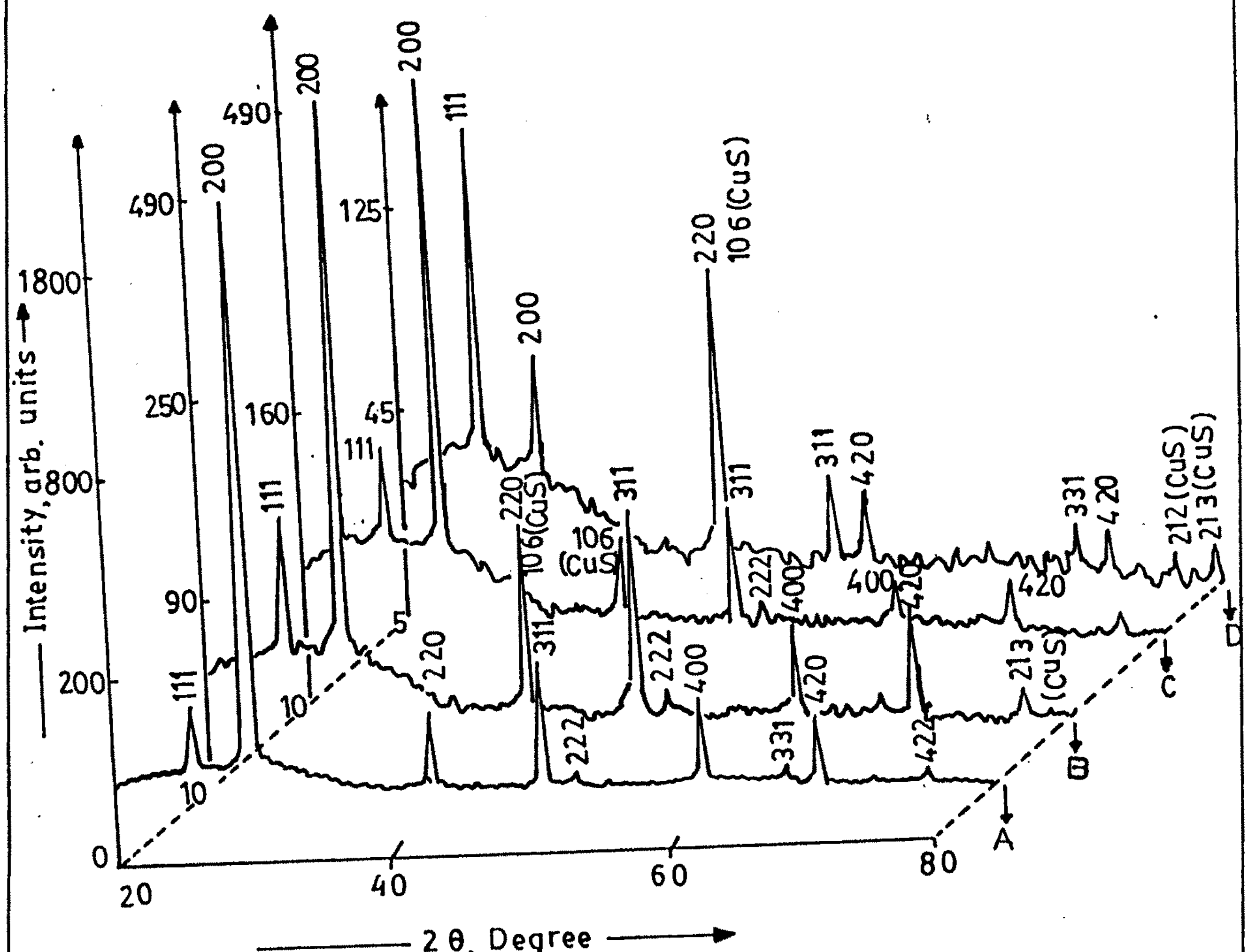

Fig. 3.6 The X - ray diffractograms of four typical PbS : Cu compositions :
A ⟶X = 0, B⟶X = 0.15, C⟶X = 0.35 and D⟶X = 0.8.

copper does not affect the formation of PbS but additionally an increasing amount of hexagonal CuS has been formed /2,11,12/.The most intense peak for pure PbS corresponds to (200) reflection and it remains as most intense up to $x \leq 0.5$. For highher values of x, peak intensity goes on decreasing continuously as x is increased. Further, the intense reflection (111) has relatively less intensity at lower values of x and it becomes most prominant above x=0.5, where the (200) reflection becomes less intense. The variation of relative intensities with the Cu-content (x) for the reflections (200) and (111) is shown in figure 3.7. It has also been found that no intense reflection corresponding to hexagonal CuS has been observed /2/. Therefore, for lower range of Cu-concentration, copper enters in to the lattice of PbS as a dopant and it does not forms an appreciable amount of solid solution with PbS /2/. For higher concentration of Cu in PbS, formation of separate phases of PbS and CuS is obvious /2,12/. Table 3.1 shows the comparison of d values and relative intensities with the ASTM values.

b) SEM studies

The crystalline nature of the PbS:CuS mixed thin films was further examined by a scanning electron microscopy technique. The SEM micrographs of six typical compositions are shown in figure 3.8. It is evident that there is a little decrease in the grain size, however, Cu-concentration has no marked effect on crystallite size /2/.

3.3.4 Optical properties

The optical absorption studies have been done on these

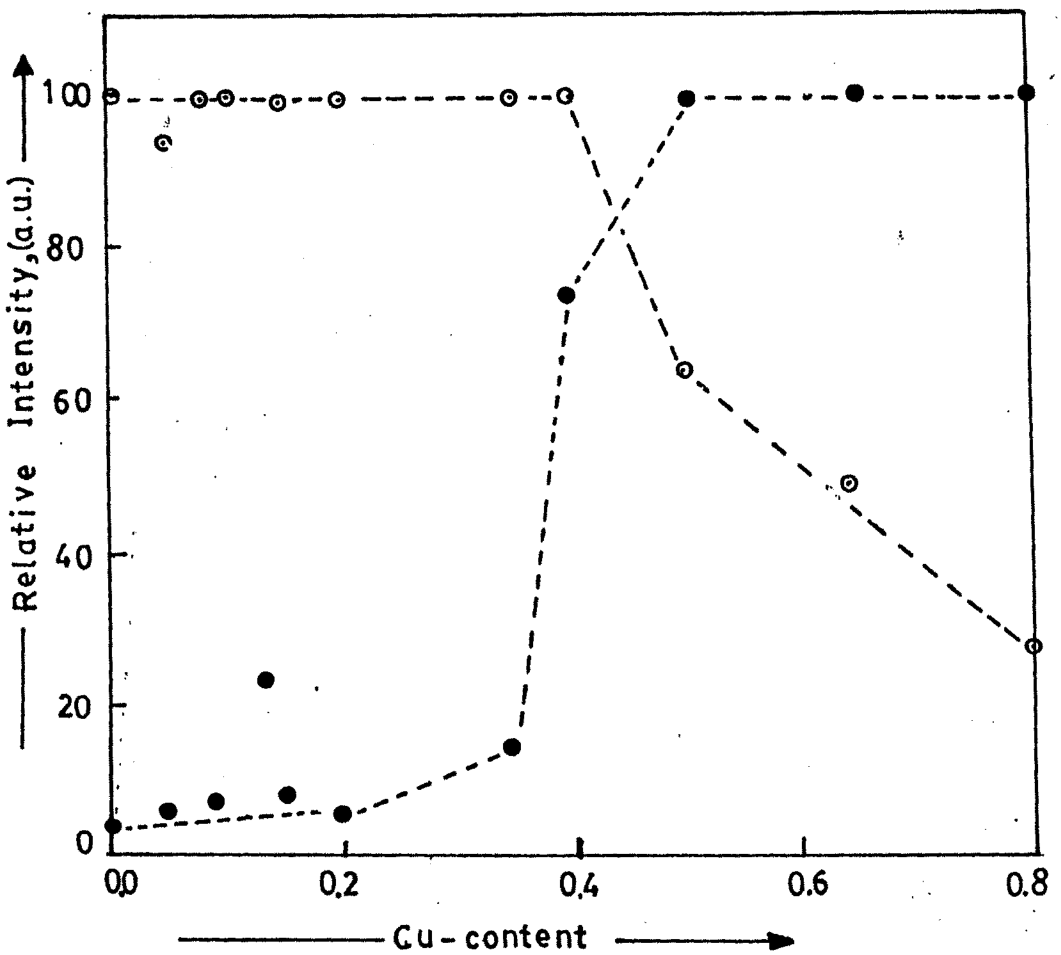

Fig. 3.7 Variation of relative intensities with the Cu-content for the reflections (200) and (111)
● →(200) , ⊙ →(111)

Table 3.1 : Comparison of observed d values, relative intensities with ASTM data of different samples.

Composition Parameter X	Observed d values (A°)	Observed I / I max	PbS [Cubic] standard d values (A°)	I / Imax	hKl	CuS (hexagonal) standard d values (A°)	I / Imax	hKl
0	3.425	4	3.429	84	111	-	-	-
	2.968	100	2.969	100	200	-	-	-
	2.097	4	2.099	57	220	-	-	-
	1.789	7.0	1.790	35	311	-	-	-
	1.708	0.5	1.714	16	222	-	-	-
	1.480	2.4	1.484	10	400	-	-	-
	1.360	0.4	1.362	10	331	-	-	-
	1.326	2.7	1.327	17	420	-	-	-
	1.209	0.3	1.212	10	422	-	-	-
	1.142	1.3	1.142	6	511	-	-	-
	1.050	0.3	1.048	3	440	-	-	-
0.05	3.428	100	3.429	84	111	-	-	-
	2.968	93.2	2.969	100	200	-	-	-
	2.097	48.0	2.099	57	220	2.097	6	106
	1.790	21.0	1.790	35	311	-	-	-
	1.712	10.2	1.714	16	222	-	-	-
	1.484	7.0	1.484	10	400	1.463	6	1010
	1.460	4.9	-	-	-	1.463	6	1010
	1.361	7.3	1.362	10	331	-	-	-
	1.326	8.1	1.327	17	420	-	-	-
	1.273	4.9	-	-	-	1.280	10	208
	1.210	4.9	1.212	10	422	1.210	10	213

Composition Parameter X	Observed d values (A°)	Observed I / I max	PbS [Cubic] standard d values (A°)	PbS I / Imax	PbS hKl	CuS (hexagonal) standard d values (A°)	CuS I / Imax	CuS hKl
0.075	3.432	79.0	3.429	84	111	-	-	-
	2.972	100	2.969	100	200	-	-	-
	2.099	96.0	2.099	57	220	2.097	6	106
	1.789	24.0	1.790	35	311	-	-	-
	1.713	9.0	1.714	16	222	-	-	-
	1.634	4.0	-	-	-	1.634	4	201
	1.484	6.0	1.484	10	400	1.463	6	1010
	1.360	9.8	1.362	10	331	1.354	8	1011
	1.327	12.8	1.327	17	420	-	-	-
	1.290	4.0	-	-	-	1.280	10	208
	1.211	6.6	1.212	10	422	1.210	10	213
	1.095	4.0	-	-	-	1.095	10	300
	1.049	4.0	1.049	3	440	-	-	-
0.1	3.432	24.0	3.429	84	111	-	-	-
	2.968	100	2.969	100	200	-	-	-
	2.100	44.0	2.099	57	220	2.097	6	106
	1.789	23.0	1.790	35	311	-	-	-
	1.712	2.2	1.714	16	222	-	-	-
	1.483	4.0	1.484	10	400	1.463	6	1010
	1.362	3.4	1.362	10	331	1.354	8	1011
	1.327	10.2	1.327	17	420	-	-	-
	1.211	3.8	1.212	10	422	1.210	10	213
	1.142	2.9	1.142	6	511	-	-	-

Composition Parameter X	Observed d values (A°)	Observed I / I max	PbS [Cubic] standard			CuS (hexagonal) standard		
			d values (A°)	I / Imax	hKl	d values (A°)	I / Imax	hKl
0.15	3.426	7.4	3.429	84	111	-	-	-
	2.969	99.5	2.969	100	200	-	-	-
	2.097	12.1	2.099	57	220	2.097	6	106
	1.789	18.6	1.790	35	311	-	-	-
	1.483	7.0	1.484	10	400	1.463	6	1010
	1.327	8.9	1.327	17	420	-	-	-
	1.211	1.9	1.212	10	422	-	-	-
	1.141	3.3	1.142	6	511	-	-	-
0.2	3.424	5.5	3.429	84	111	-	-	-
	2.969	100	2.969	100	200	-	-	-
	2.096	4.8	2.099	57	220	2.097	6	106
	1.790	7.4	1.790	35	311	-	-	-
	1.484	2.9	1.484	10	400	1.463	6	1010
	1.357	0.82	1.362	10	331	1.354	8	1011
	1.338	87	1.327	17	420	-	-	-
	1.327	3.0	1.327	17	420	-	-	-
	1.141	1.0	1.142	6	511	-	-	-

Composition Parameter X	Observed d values (A°)	Observed I / I max	PbS [Cubic] standard d values (A°)	PbS I / Imax	PbS hKl	CuS (hexagonal) standard d values (A°)	CuS I / Imax	CuS hKl
0.35	3.426	14.8	3.429	84	111	-	-	-
	2.969	100	2.969	100	200	-	-	-
	2.097	9.9	2.099	57	220	2.097	6	106
	1.789	9.7	1.790	35	311	-	-	-
	1.714	1.9	1.714	16	222	-	-	-
	1.483	3.4	1.484	10	400	1.463	6	1010
	1.326	3.4	1.327	17	420	-	-	-
	1.210	1.8	1.212	10	422	1.210	10	213
	1.143	1.5	1.142	6	511	-	-	-
	1.093	8.0	-	-	-	1.095	10	300
0.4	3.426	14.79	3.429	84	111	-	-	-
	2.969	100	2.969	100	200	-	-	-
	2.097	9.95	2.099	57	220	2.097	6	106
	1.789	9.71	1.790	35	311	-	-	-
	1.715	1.92	1.714	16	222	-	-	-
	1.483	3.41	1.484	10	400	1.463	6	1010
	1.326	3.41	1.327	17	420	-	-	-
	1.210	1.81	1.212	10	422	1.210	10	213
	1.143	1.51	1.142	6	511	-	-	-
	1.018	1.51	-	-	-	1.012	8	306

Composition Parameter X	Observed d values (A°	Observed I / I max	PbS [Cubic] standard d values (A°)	PbS I / Imax	PbS hKl	CuS (hexagonal) standard d values (A°)	CuS I / Imax	CuS hKl
0.5	3.430	100	3.429	84	111	-	-	-
	2.970	64	2.969	100	200	-	-	-
	2.101	79.72	2.099	57	220	-	-	-
	2.098	84.90	2.099	57	220	-	-	-
	1.789	23.59	1.790	35	311	-	-	-
	1.712	7.76	1.714	16	222	-	-	-
	1.363	6.98	1.362	10	331	-	-	-
	1.346	5.22	-	-	-	1.343	6	207
	1.327	9.00	1.327	17	420	-	-	-
	1.212	5.90	1.212	10	422	1.210	10	213
	1.093	-	-	-		1.095	10	300
0.65	3.433	100	3.429	84	111	-	-	-
	2.970	34.28	2.969	100	200	-	-	-
	2.098	59.25	2.099	57	220	-	-	-
	1.788	13.09	1.790	35	311	-	-	-
	1.711	12.16	1.714	16	222	-	-	-
	1.549	5.0	-	-	-	1.550	5.9	116
	1.360	5.6	1.362	10	331	-	-	-
	1.326	6.25	1.327	17	420	-	-	-
	1.210	4.43	1.212	10	422	1.210	10	213
	1.094	3.91	-	-	-	1.095	10	300

Composition Parameter X	Observed d values (A°)	Observed I / I max	PbS [Cubic] standard			CuS (hexagonal) standard		
			d values (A°)	I / Imax	hKl	d values (A°)	I / Imax	hKl
0.8	3.428	100	3.429	84	111	-	-	-
	2.966	27.70	2.969	100	200	-	-	-
	2.100	59.25	2.099	57	220	-	-	-
	1.790	13.09	1.790	35	311	-	-	-
	1.712	12.16	1.714	16	222	-	-	-
	1.540	5.00	-	-	-	1.550	35	116
	1.361	6.93	1.362	10	331	-	-	-
	1.326	6.25	1.327	17	420	-	-	-
	1.230	4.43	-	-	-	1.227	6	212
	1.210	4.43	1.212	10	422	1.210	10	213
	1.012	4.43	-	-	-	1.012	8	306

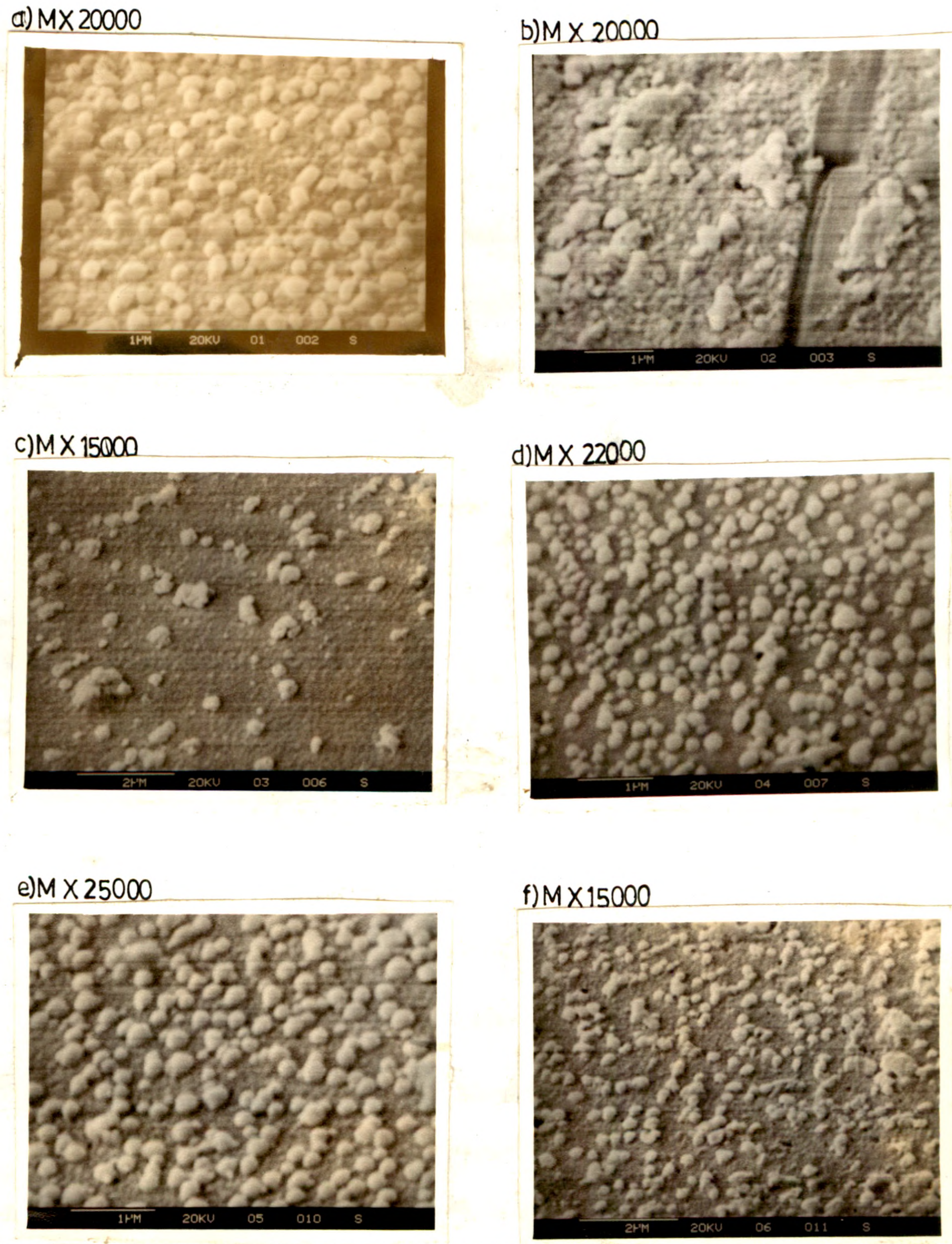

Fig. 3.8 SEM micrographs of :

a) Pure PbS, b) X = 0.075, c) X = 0.1, d) X = 0.2, e) X = 0.35 and f) X = 0.5.

samples. The range of wavelength used was from 5000 A° to 26000 A° [redacted]. The optical absorption coefficient (α) was determined from these observations and its wavelenth dependence is shown in figure 3.9. The absorption spectra show clearly three absorption edges for pure PbS and two for PbS:Cu samples /2,12/. These are at 0.45 eV, 0.90 eV and 1.8 eV, respectively. The absorption edges at 0.45 eV and 1.8 eV are due to the fundamental optical transitions in PbS as is reported by Deshmukh et al /1,2/ and Reddy et al /20/ for $(CdS)_x(PbS)_{1-x}$ composite thin films. The absorption edge at 0.90 eV might be due to the mixed phase of PbS and CuS; of course we cannot restrict a negligibly small amount of solid solution formation between the phases /2,12,21/. If we see keenly on the energy axis, a little variation in band gap has also been observed supporting the above statements. The plots of $(\alpha h\nu)^2$ vs $h\nu$ are shown in figure 3.10. The transitions are also of the direct type.

3.4 Conclusions

A novel way of obtaining PbS:CuS mixed thin films using a modified chemical deposition process is presented.Good quality deposition with extremely less consumption of both an electrical power and the active materials is made possible. The deposits are pleasant in colour and therefore the material is one of the best suited for solar control applications (for architectural glazings, decorative purposes etc). Both PbS and PbS:CuS samples are crystalline in nature and pure PbS is cubic in structure while mixed samples contain both cubic PbS and hexagonal CuS phases /2,11,21/.Optical studies showed three absorption edges for PbS and two for PbS:CuS samples /2,21/. Thus the XRD, SEM and

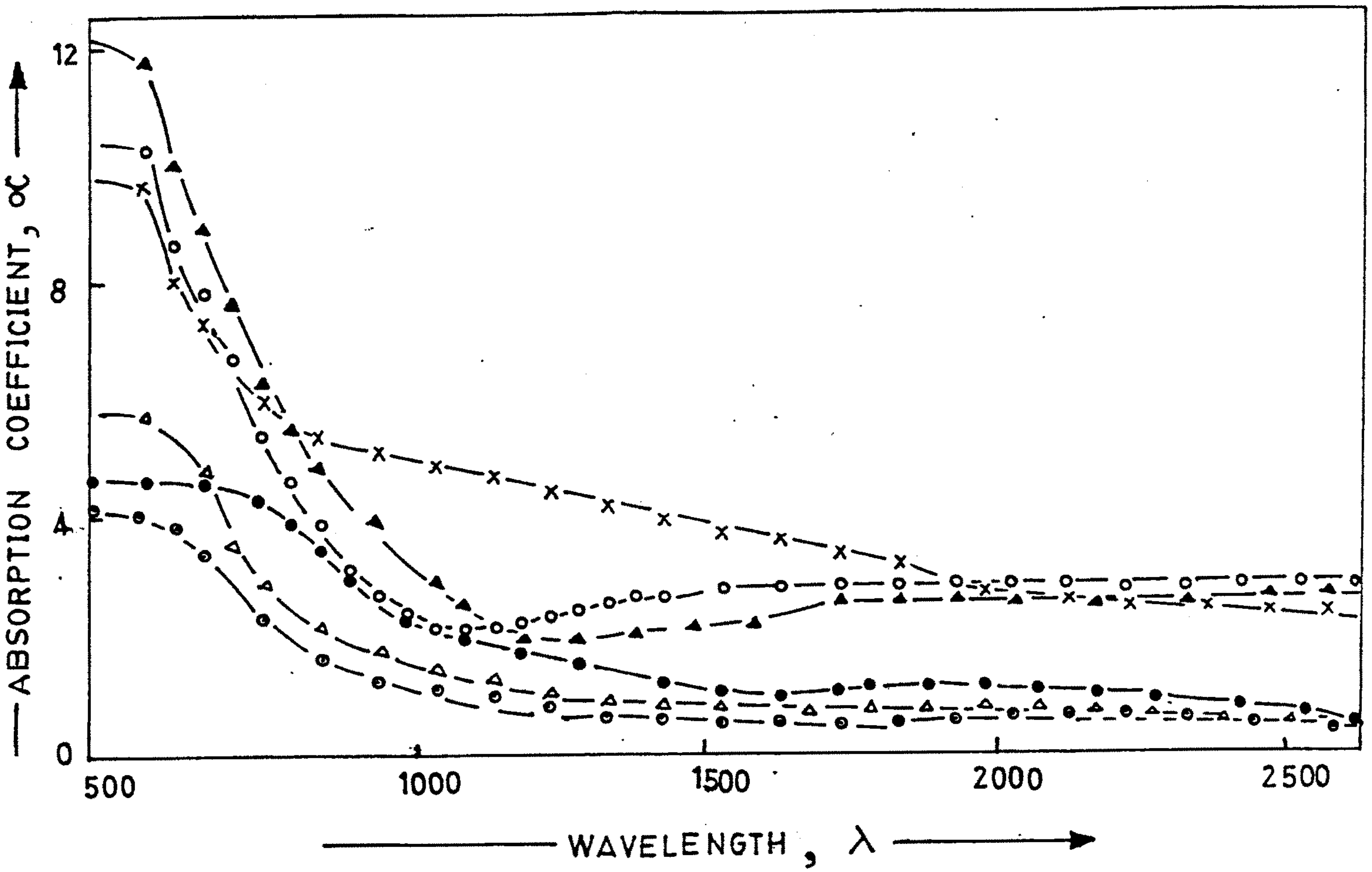

Fig. 3.9 Wavelength dependence of optical absorption coefficient :
● → X = 0, ⊙ → X = 0.075, △ → X = 0.2, O → X = 0.5, ▲ → X = 0.4,
x → X = 0.8.

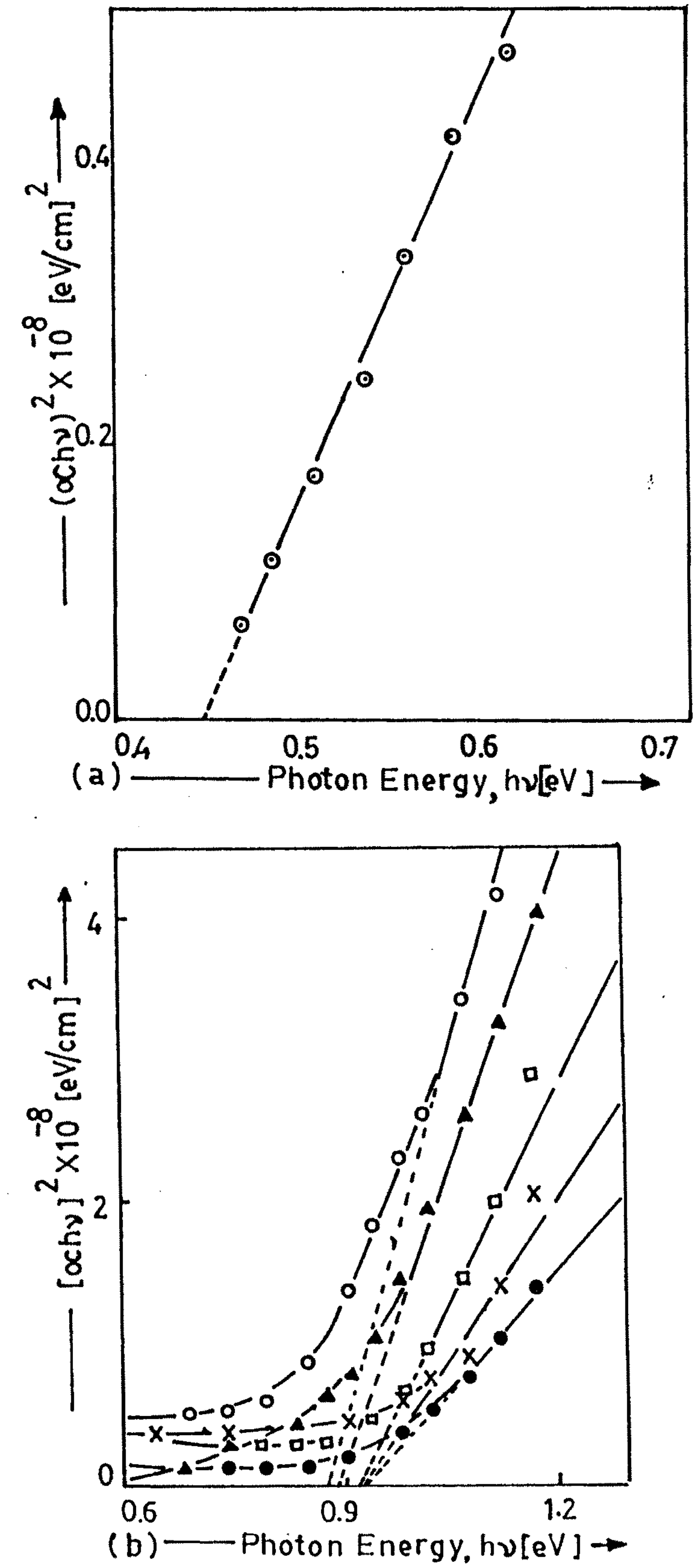

Fig.3.10(a) and (b) Optical band gap determination for different PbS : Cu compositions :
a) ⊙ → Pure PbS, b) O → X = 0, ● → X = 0.075, □ → X = 0.1, ▲ → X = 0.15 and X → X = 0.2.

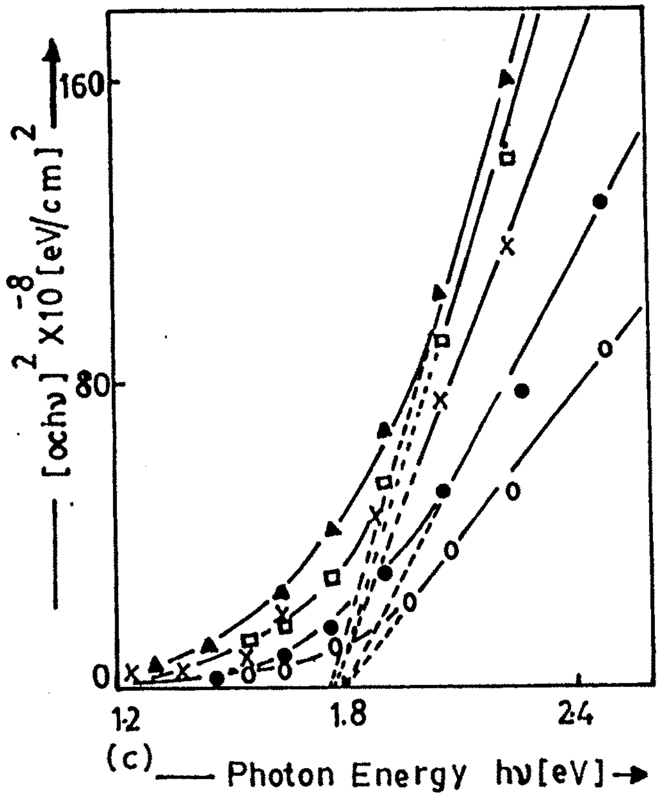

Fig. 3.10 (c) Optical band gap determination for different PbS : Cu compositions : O $\longrightarrow$ X = 0.05, ● $\longrightarrow$ X = 0.075, □ $\longrightarrow$ X = 0.1, ▲ $\longrightarrow$ X = 0.15 and x $\longrightarrow$ X = 0.2.

optical studies revealed that cubic PbS does not allow CuS to form a solid solution through out the range of interest. Further there is no continuous change in the optical energy gap and the lattice constants as a result of introduction of Cu in PbS indicating that the samples are of the mixed composite type /1,2,20,22/. The electrical conductivity and the TEP studies showed p-type conduction. The carrier concentration is of the order of 10^{19} cm^{-3}. The electrical conductivity increases considerably for a very small amount of Cu-concentration added in PbS which can be considered advantageous for solar cell applications.

REFERENCES

1. L.P.Deshmukh, B.M.More, S.G.Holicatti and P.P.Hankare, Bull. Mater. Sci., 17 (1994) 455
2. L.P.Deshmukh, H.D.Patil, S.G.Holikatti and B.M.More, Bull. Electrochem. (In press)
3. J.E.Bauerie, P.H.Sutter and R.W.Ure, Jr. in "Thermoelectricity Science and Technology", (ed) R.R. Heikel and R.W.Ure, Jr. Interscience Publishers, (1969) P.285
4. L.P.Deshmukh, S.G.Holikatti and P.P.Hankare, J. Phys. D: Appl., phys, 27 (1994) 1786
5. V.M.Garcia, M.T.S.Nair and P.K.Nair, Solar Energy Mat; 23 (1991) 47
6. K.L.Chopra, R.C.Kainthala, D.K.Pandya and A.P.Thakoor, Physics of Thin Films, (eds) G Hass et al, N.Y. 12 (1982) P.201
7. C.V.Suryanarayana,A.S.Lakshmanan, V.Subramanian and R.K.Kumar, Bull. Electrochem; 2 (1986) 57
8. L.P.Deshmukh, A.B.Palwe and V.S.Sawant, Sol. Ener. Mat., 20 (1990) 341
9. L.P.Deshmukh, K.V.Zipre, A.B.Palwe, B.P.Rane, P.P.Hankare and A.H.Manikshete, Sol.Ener.Mat. & Sol. Cells, 28 (1992) 249
10. G.Gordillo, Sol. Ener. Mat. and Sol. Cells, 25(1992) 41
11. T.P.Sharma, R.Kumar and G. Jain, Ind. J. Pure and Appl. Phys; 29 (1991) 583
12. L.P.Deshmukh, H.D.Patil, S.G.Holikatti and B.M.More, Proc. Fifth Int. Symp. on Advances in Electrochemical Science and Technology, 24 - 26 Nov. 1994 Madras, India P.No.7.15
13. J.George, T.I.Palson and K.S.Joseph, Solid State Commun., 58, (1986) 605

14. L.I.Bytenskii, T.S.Gudkin, E.K.Iordanishvili, S.A.Kazmin, V.I.Kuidanov, S.A.Nemov and Yu.I. Ravich, Sov. Phys. Semicond., 11 (1977)894

15. T.S.Gudkin, I.A.Drabkin, V.I.Kaidanov and O.G.Sterlyadkina, Sov. Phys. Semicond., 8 (1975) 453

16. L.N. Neustroev and V.V.Osipov, Soc. Phys. Semicond., 18(1984) 224

17. S.Espevic, Chen-ho-Wu and R.H.Bube, J.Appl. Phys; 42 (1971) 3513

18. Cook Jr. Thesis " The CuS phase diagram", Gould Labs, Cleveland, Ohio

19. Swanson and Fuyat, NBS circular, 539, Vol.II (1953) 18

20. G.B.Reddy, D.K.Pandya and K.L.Chopra, Sol. Ener. Mat., 15(1987) 383

21. L.P.Deshmukh, H.D.Patil, G.S.Shahane and R.N.Mulik, Mat. Chem. Phys. (Communicated)

22. L.P.Deshmukh, S.G.Holikatti and B.M.More, Mat.Chem.Phys., 39(1995) 278